Ultrasound-Induced Calcium Oscillations and Waves in Chinese Hamster Ovary Cells in the Presence of Microbubbles

R. E. Kumon,*† M. Aehle,† D. Sabens,† P. Parikh,† D. Kourennyi,† and C. X. Deng*†
*Department of Biomedical Engineering, University of Michigan, Ann Arbor, Michigan; and †Department of Biomedical Engineering, Case Western Reserve University, Cleveland, Ohio

ABSTRACT This study investigated the effects of ultrasound on the intracellular [Ca^{2+}] of Chinese hamster ovary cells in the presence of albumin-encapsulated Optison microbubbles. Cells were exposed to 1 MHz ultrasound (tone burst of 0.2 s duration, 0.45 MPa peak pressure) while immersed in solution of 0.9 mM Ca^{2+}. Calcium imaging of the cells was performed using digital video fluorescence microscopy and Ca^{2+}-indicator dye fura-2AM. Experimental evidence indicated that ultrasound caused a direct microbubble-cell interaction resulting in the breaking and eventual dissolution of the microbubble and concomitant permeabilization of the cells to Ca^{2+}. These cells exhibited a large influx of Ca^{2+} over 3–4 s and did not return to their equilibrium levels. Subsequently, some cells exhibited one or more Ca^{2+} oscillations with the onset of oscillations delayed by 10–80 s after the ultrasound pulse. A variety of oscillations were observed including decaying oscillations returning to the baseline value over 35–100 s, oscillations superimposed on a more gradual recovery over 150–200 s, and oscillations continued with increased amplitude caused by a second ultrasound tone burst. The delays in onset appeared to result from calcium waves that propagated across the cells after the application of the ultrasound pulse.

Received for publication 22 May 2007 and in final form 27 June 2007.

Address reprint requests and inquiries to Cheri X. Deng, Tel: 734-936-2855; Fax: 734-936-1905;
E-mail: cxdeng@umich.edu.

Mechanical stresses on cells due to direct contact (1), fluid flow (2), and ultrasound (US) (3) induce intracellular [Ca^{2+}] ([Ca^{2+}]$_i$) transients. In particular, sonoporation, or US-induced plasma membrane poration, is facilitated and increased by the use of microbubbles in the extracellular solution, thereby enhancing its potential for intracellular drug and gene delivery (4). In addition, Ca^{2+} plays an important role in cell recovery after sonoporation (5). Recent studies using calcium imaging show US-induced increases in [Ca^{2+}]$_i$ in various types of cells (6–10). In this study we report the observation of [Ca^{2+}]$_i$ oscillations and waves induced by US in Chinese hamster ovary (CHO) cells in a solution containing microbubbles.

CHO cells are a line of epithelial-like cells widely used as a mammalian cell model. For our experiments, the cells were grown in culture dishes for 3 days following standard protocols. As described previously (8), the cells were first loaded in darkness with a 5-μM fura-2 AM (Invitrogen, Carlsbad, CA) solution for 60 min. Next, the cells were washed and immersed in a phosphate-buffered solution with [Ca^{2+}]$_o$ = 0.9 mM at room temperature and placed under the microscope for online measurement. One or more 1 MHz tone bursts (0.2 s, 0.45 MPa) were applied to the cells using an US transducer (Panametrics, Waltham, MA) with its 3/4-inch active element immersed in solution in the absence or presence of 5% Optison (GE Healthcare, Princeton, NJ), an US imaging contrast agent consisting of albumin-encapsulated C_3F_8 gas bubbles ($\sim$3 μm mean diameter). For fura-2 ratiometric imaging, the cells were excited alternatingly with light at 380 and 340 nm from a Xe lamp, and the emission images filtered at 510 nm were acquired using an inverted microscope (Nikon TE-300, Melville, NY) with a cooled charge-coupled device camera (Photometrics Coolsnap HQ, Tucson, AZ) in pairs every $\sim$0.63 s continuously for the duration of the experiment.

Fig. 1 shows a series of cell images with 380 nm excitation when US was applied at 30.0 s. The image at 31.0 s shows dark spots (*arrows*) and reduced fluorescence intensity within two adjacent cells (*open arrows*). The corresponding 340 nm images (not shown) increased in brightness in the same cells, indicating an increase in ratio $R = F_{340}/F_{380}$ and thereby [Ca^{2+}]$_i$ after the US pulse. No changes in [Ca^{2+}]$_i$ were observed in our experiment without US or with US in the absence of Optison.

We interpret the dark spots to be the remaining gas cores of Optison that have been destroyed by the US pulse. We believe that they are not intact Optison because: i), they did not appear to fluoresce like other Optison (cf. Fig. 2); and ii), they appeared to rapidly ($<$3 s) dissolve into the fluid. Optison would be expected to fluoresce at visible wavelengths given that it is encapsulated by shells of human serum albumin (11). Moreover, recent studies suggest that residual gas cores can result from US-treated Optison adjacent to a cellular monolayer (12), and US-destroyed Optison dissolve within a few seconds (13).

Fig. 2 shows the ratio R of the spatial mean fluorescence intensities within a cell as a function of time for several sets of cells. US pulses were applied at 30 and 210 s. Fig. 2 *A* shows the ratio plots of two of the cells in Fig. 1. One cell (*red*) appeared to directly interact with the microbubbles,

Editor: Herbert Levine.

doi: 10.1529/biophysj.107.113365

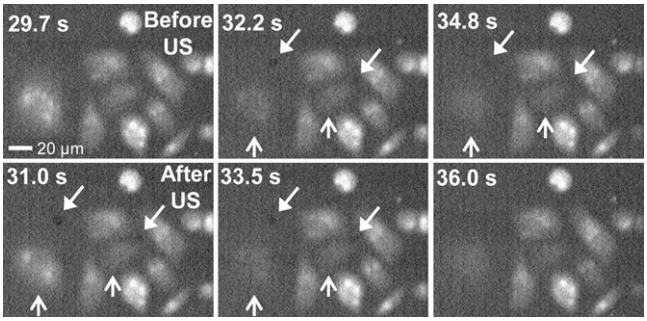

FIGURE 1 Fluorescence images of CHO cells loaded with fura-2 AM before and after ultrasound (*US*) treatment (380-nm excitation, filtered 510-nm emission) in $[Ca^{2+}] = 0.9$ mM solution. The arrows point to microbubbles that appear after the US is applied. The cells (*open arrows*) to the left of the bubbles darken, indicating increased intracellular $[Ca^{2+}]$. The microbubbles eventually dissolve into the surrounding fluid.

resulting in an influx of Ca^{2+} such that the $[Ca^{2+}]_i$ did not recover. (The noisy signal in the ratio results from the 380 nm intensities being close to the background level.) Rise time to the maximum was 3–4 s. In contrast, a nearby cell experienced a transient rise in $[Ca^{2+}]_i$ after a delay of 10 s but eventually recovered after 140 s. Fig. 2 *B* shows similar response by cells in a separate area of the dish initiated by different microbubbles. Rise time to the peak was 3–4 s. Time of recovery to equilibrium $[Ca^{2+}]_i$ for shown adjacent cells ranged from 35 to 100 s.

We observed that many cells experience their initial peak in $[Ca^{2+}]_i$ after the US pulse has ended, and their recoveries exhibited different dynamic behaviors. Fig. 2, *C* and *D*, show examples of cells with decaying $[Ca^{2+}]_i$ transients with oscillations. The cells showed an increase in $[Ca^{2+}]_i$ over 3–4 s and then decayed back to equilibrium over 150–200 s, with a delayed onset of 8–10 s from the US application. The observed period of the oscillations ranged from 20 to 30 s. In general, the oscillations tend to extend the recovery time. The increase after the second US pulse was less than the first. Fig. 2 *E* shows transients with the oscillations sustained by the second US pulse. This effect was less commonly observed than those shown in Fig. 2, *C* and *D*. Panel *F* shows the initiation of oscillations in cells far from the region of direct microbubble interaction. The onset of the oscillations was much delayed, up to 80 s for one cell. The oscillations had comparable amplitude and period (~20 s) to those in Fig. 2, *C–E*, but were nearly in phase for adjacent cells. In addition, one cell had only single cycle of oscillation, whereas another ''skipped'' an oscillation cycle relative to its neighbor. In all the cases shown except Fig. 2 *E*, the $[Ca^{2+}]_i$ response to the second US pulse occurred after a 20–60 s delay. Finally, Fig. 2 *G* shows a background-corrected 380-nm image before US exposure. Several intact Optison bubbles are seen quite clearly and remained easily visible after US exposure, in contrast to the bubbles seen in Fig. 1.

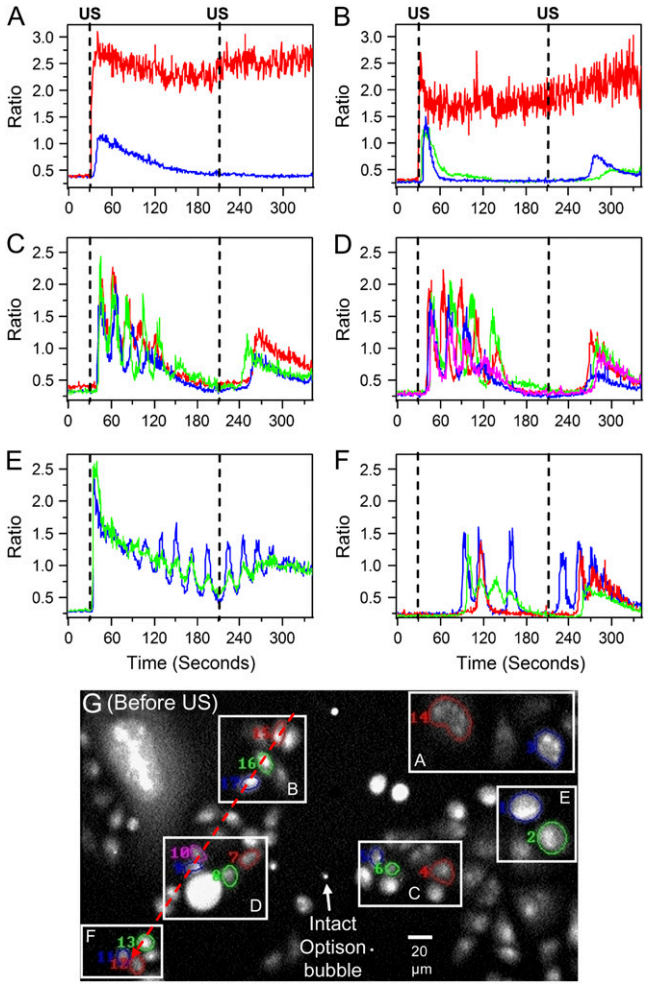

FIGURE 2 US-induced $[Ca^{2+}]_i$ oscillations in CHO cells in the same field of view. The cells are immersed in $[Ca^{2+}]_o = 0.9$ mM solution for two US pulses applied at 30 and 210 s. (*A*, *B*) Cells that do not recover or show decay to baseline. (*C*, *D*) Cells with slower decay to baseline and superimposed oscillations. (*E*) Cells with superimposed oscillations sustained by the second ultrasound pulse. (*F*) Cells with oscillations of one, two, and three cycles with smaller or no underlying transient. (*G*) Background-corrected image with map of manually segmented cells shown in graphs *A–F*.

The delays between the US pulses and the calcium responses of many cells appeared to result from propagating waves. Fig. 3 *A* shows a 380-nm image with a line drawn across the set of cells corresponding to the dashed red line in Fig. 2 *G*. Fig. 3 *B* shows a ''linescan'' image, which is constructed by recording the ratio value at locations along the line drawn in Fig. 3 *A* at each time point. The value of the ratio is color-coded and modulated by the intensity of the 340-nm images to suppress image noise in background. The linescan shows a wave traveling from right to left, or from region B through D, to F, in Fig. 2 *G*. The initial velocity of the wave (10–12 μm/s) slowed significantly when the wave encountered a larger cell (*bright spot* in image). A similar wave that

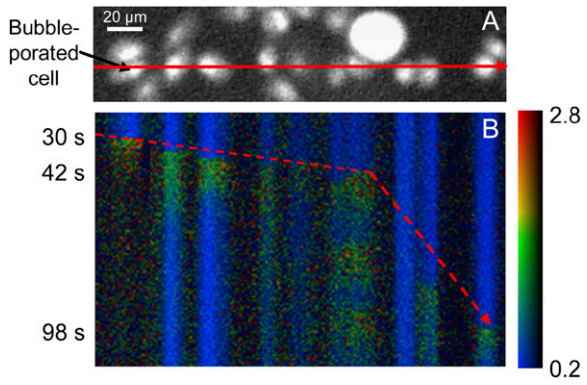

FIGURE 3 [Ca^{2+}] waves and oscillations in CHO cells immersed in [Ca^{2+}] = 0.9 mM solution stimulated by an ultrasound pulse at 30 s. (*A*) Definition of tracking line on 380-nm image. (*B*) Intensity-modulated display of ratio as a function of time along the line shown in image *A*. The dashed line is added as a guide to show the delayed initiation.

propagated after the second US pulse (data not shown) was found to correlate with the delays seen in Fig. 2 after 210 s.

Based on these results, we hypothesize that the cells that do not recover in Fig. 2, *A* and *B*, are irreversibly porated by US-bubble interactions, such as microjets from asymmetric bubble collapse or ballistic shell-fragment penetration (12), and the subsequently delayed $[Ca^{2+}]_i$ response by adjacent cells is the result of calcium waves originating from the cells porated by the microbubbles. Suggested mechanisms for mechanically induced calcium oscillations and waves include the propagation of second messengers like IP_3 through gap junctions and activation of receptors on adjacent cells following release of paracrine factors into the extracellular space, with the specific mechanism varying with cell type and species (14). Calcium wave speed propagation via gap junctions has been typically reported in the range of 10–30 μm/s (14), which encompasses the initial speed seen in Fig. 3. Although the observed movement of intact bubbles indicated weak fluid movement (<2 μm/s) from Optison mixing and US streaming, it was not correlated with the direction of wave propagation. Calcium wave propagation also appears to have occurred across regions around cells that did not show changes in $[Ca^{2+}]_i$ and across regions without cells, suggesting a paracrine factor in these cases. In epithelial airway cells, direct mechanical stimulation after ATP stimulation was shown to increase the amplitude of subsequent oscillations (15), similar to Fig. 2 *E*. However, still other mechanisms may be at work. For example, it has been shown that in cells exposed to microbubbles H_2O_2 and Ca^{2+} can be increased using US of comparable amplitude to this study, though with pulsed US and 10-s exposure time (9). Furthermore, introduction of catalase, an H_2O_2 scavenger, reduced the Ca^{2+} influx, suggesting that reactive oxygen species may also play a role in membrane permeabilization.

Although we concentrated on measurements from one set of measurements in this letter, experiments on nine more sets of cells with $[Ca^{2+}]_o = 0.9$ mM or 2.5 mM showed similar oscillations and waves. Experiments with $[Ca^{2+}]_o = 0$ mM showed no oscillations or waves. Additional work is necessary to elucidate the mechanisms of US-induced changes in intracellular calcium activities in CHO cells and other cell types. Investigation of these mechanisms will be important for understanding the bioeffects of US in various applications including intracellular drug and gene delivery via US.

ACKNOWLEDGMENTS

The authors acknowledge Yun Zhou and Grant Steyer for technical advice and Olivier Izad for cell culturing.

This work was supported in part by the American Cancer Society Institutional Research Grant to Case Western Reserve University and National Institutes of Health grant No. R01CA116592.

REFERENCES and FOOTNOTES

1. Furuya, K., K. Enomoto, and S. Yamagishi. 1993. Spontaneous calcium oscillations and mechanically and chemically induced calcium responses in mammary epithelial cells. *Pflügers Archiv Eur. J. Physiol.* 422:295–304.
2. Yellowley, C. E., C. R. Jacobs, Z. Li, Z. Zhou, and H. J. Donahue. 1997. Effects of fluid flow on intracellular calcium in bovine articular chondrocytes. *Am. J. Physiol. Cell Physiol.* 273:C30–C36.
3. Mortimer, A. J., and M. Dyson. 1988. The effect of therapeutic ultrasound on calcium uptake in fibroblasts. *Ultrasound Med. Biol.* 14:499–506.
4. Miller, D. L., S. V. Pislaru, and J. F. Greenleaf. 2002. Sonoporation: mechanical delivery by ultrasonic cavitation. *Som. Cell Mol. Genetics.* 27:115–134.
5. Deng, C. X., F. Sieling, H. Pan, and J. Cui. 2004. Ultrasound-induced cell membrane porosity. *Ultrasound Med. Biol.* 30:519–526.
6. Parvizi, J., V. Parpura, J. F. Greenleaf, and M. E. Bolander. 2002. Calcium signaling is required for ultrasound-stimulated aggrecan synthesis by rat chondrocytes. *J. Orthop. Res.* 20:51–57.
7. Kono, T., T. Nishikora, H. Kataoka, Y. Uchio, M. Ochi, and K. Enomoto. 2006. Spontaneous oscillation and mechanically induced calcium waves in chondrocytes. *Cell Biochem. Funct.* 24:103–111.
8. Sabens, D., M. Aehle, G. Steyer, D. Kourennyi, and C. X. Deng. 2006. Calcium imaging of sonoporation of mammalian cells. *In* Therapeutic Ultrasound: 5th ISTU. G. J. Clement, N. J. McDannold, and K. Hynynen, editors. AIP Press, New York. 533–537.
9. Juffermans, L. J. M., P. A. Dijkmans, R. J. P. Musters, C. A. Visser, and O. Kamp. 2006. Transient permeabilization of cell membranes is related to formation of hydrogen peroxide. *Am. J. Physiol. Heart Circ. Physiol.* 291:H1595–H1601.
10. Kumon, R. E., P. Parikh, D. Sabens, M. Aehle, D. Kourennyi, and C. X. Deng. 2007. Measuring and modeling sonoporation dynamics in mammalian cells via calcium imaging. *In* Therapeutic Ultrasound: 6th ISTU. C.-C. Coussios and G. ter Haar, editors. AIP Press, New York. 484–490.
11. Amisha Kamal, J. K., and D. V. Behere. 2002. Spectroscopic studies on human serum albumin and methemalbumin: optical, steady-state, and picosecond time-resolved fluorescence studies, and kinetics of subtrate oxidation by methemalbumin. *J. Biol. Inorg. Chem.* 7:273–283.
12. Prentice, P., A. Cuschieri, K. Dholakia, M. Prausnitz, and P. Campbell. 2005. Membrane disruption by optically controlled microbubble cavitation. *Nature Phys.* 1:107–110.
13. Chomas, J. E., P. Dayton, J. Allen, K. Morgan, and K. W. Ferrara. 2001. Mechanisms of contrast agent destruction. *IEEE Ultrason. Ferroelec. Freq. Control.* 48:232–248.
14. Falcke, M. 2004. Reading the patterns of living cells—the physics of Ca^{2+} signaling. *Adv. Phys.* 53:255–440.
15. Evans, J. H., and M. J. Sanderson. 1999. Intracellular calcium oscillations induced by ATP in airway epithelial cells. *Am. J. Physiol. Lung Cell. Mol. Physiol.* 277:L30–L41.